

REPORT DOCUMENTATION PAGE

Form Approved
OMB No. 0704-0188

Public reporting burden for this collection of information is estimated to average 1 hour per response, including the time for reviewing instructions, searching existing data sources, gathering and maintaining the data needed, and completing and reviewing this collection of information. Send comments regarding this burden estimate or any other aspect of this collection of information, including suggestions for reducing this burden to Department of Defense, Washington Headquarters Services, Directorate for Information Operations and Reports (0704-0188), 1215 Jefferson Davis Highway, Suite 1204, Arlington, VA 22202-4302. Respondents should be aware that notwithstanding any other provision of law, no person shall be subject to any penalty for failing to comply with a collection of information if it does not display a currently valid OMB control number. **PLEASE DO NOT RETURN YOUR FORM TO THE ABOVE ADDRESS.**

1. REPORT DATE (DD-MM-YYYY) 4 June 2015		2. REPORT TYPE Conference Paper		3. DATES COVERED (From - To) 18 May 2015 – 4 June 2015	
4. TITLE AND SUBTITLE Combustion Enhancement of Liquid Fuels via Nanoparticle Additions: Screening, Dispersion, and Characterization				5a. CONTRACT NUMBER FA9300-13-M-1008	
				5b. GRANT NUMBER	
				5c. PROGRAM ELEMENT NUMBER	
6. AUTHOR(S) J.E. Boyer, Z. Bushman, J. Adair, K. Kuo, M. Billingsley				5d. PROJECT NUMBER	
				5e. TASK NUMBER	
				5f. WORK UNIT NUMBER Q13W	
7. PERFORMING ORGANIZATION NAME(S) AND ADDRESS(ES) Air Force Research Laboratory (AFMC) AFRL/RQRC 10 E. Saturn Blvd Edwards AFB, CA 93524-7680				8. PERFORMING ORGANIZATION REPORT NO.	
9. SPONSORING / MONITORING AGENCY NAME(S) AND ADDRESS(ES) Air Force Research Laboratory (AFMC) AFRL/RQR 5 Pollux Drive Edwards AFB, CA 93524-7048				10. SPONSOR/MONITOR'S ACRONYM(S)	
				11. SPONSOR/MONITOR'S REPORT NUMBER(S) AFRL-RQ-ED-TP-2015-187	
12. DISTRIBUTION / AVAILABILITY STATEMENT Approved for public release; distribution unlimited					
13. SUPPLEMENTARY NOTES For presentation at 62nd JPM / 10th MSS / 8th LPS / 7th SPS Joint Subcommittee Meeting in Nashville, TN (June 2015) PA Case Number: #15287; Clearance Date: 28 May 2015					
14. ABSTRACT Addition of nano-sized combustible particles to liquid propulsion fuel (e.g., RP-2) offers the possibility of generating an enhanced fuel with increased energy density, while maintaining or improving ignition characteristics of the bulk fuel. The culmination of increases in widespread availability/ affordability of a large variety of nano-sized particles, understanding of nano-sized particle ignition and combustion, and advances in colloidal science of nano-sized metal particle/liquid suspensions, now allow for the development of enhanced nano-fluid fuels. To evaluate the suitability of various nanoparticles for use in an enhanced fuel, it is necessary to evaluate the both physical requirements for creating a stable suspension and the compliance of readily and economically available nanopowder materials with these criteria. In addition, a suitable dispersant must be found to ensure the suspension remains stable. In this program, an initial particle and dispersant screening process was developed and reduced to a standard procedure with evaluation criteria. Multiple dispersants and particles were assessed as dilute suspensions, and the most promising dispersant compounds and concentrations identified and used for further investigation with higher particle loading fractions. Although the manufacturers' advertised specifications fell within the size criterion for forming a stable suspension, all commercially available nano-sized aluminum particles examined were found to be unsuitable in the as-delivered state. A high fraction of the particles were determined to be in the form of undispersable permanent agglomerates made up of many primary particles, represented as an Average Agglomeration Number (AAN) significantly greater than 10. After removal of the oversized agglomerates through settling and filtration, only an unacceptably small percentage of material remained in the dispersed state (often >90% loss). Therefore, initial steps were made in assessing and testing additional processing procedures (i.e., filtering, milling, etc.) that would be necessary to generate a suitable long-term stable colloidal suspension.					
15. SUBJECT TERMS N/A					
16. SECURITY CLASSIFICATION OF:			17. LIMITATION OF ABSTRACT	18. NUMBER OF PAGES	19a. NAME OF RESPONSIBLE PERSON
a. REPORT	b. ABSTRACT	c. THIS PAGE			19b. TELEPHONE NO (include area code)
Unclassified	Unclassified	Unclassified	SAR	25	N/A

COMBUSTION ENHANCEMENT OF LIQUID FUELS VIA NANOPARTICLE ADDITIONS: SCREENING, DISPERSION, AND CHARACTERIZATION

J. Eric Boyer, Zachary Bushman, and James H. Adair
Pennsylvania State University, University Park, PA

Kenneth K. Kuo
Combustion Propulsion and Ballistic Technology Corporation, State College, PA

Matthew C. Billingsley
Air Force Research Laboratory, Edwards Air Force Base, CA

ABSTRACT

Addition of nano-sized combustible particles to liquid propulsion fuel (e.g., RP-2) offers the possibility of generating an enhanced fuel with increased energy density, while maintaining or improving ignition characteristics of the bulk fuel. The culmination of increases in widespread availability/affordability of a large variety of nano-sized particles, understanding of nano-sized particle ignition and combustion, and advances in colloidal science of nano-sized metal particle/liquid suspensions, now allow for the development of enhanced nano-fluid fuels. To evaluate the suitability of various nanoparticles for use in an enhanced fuel, it is necessary to evaluate the both physical requirements for creating a stable suspension and the compliance of readily and economically available nanopowder materials with these criteria. In addition, a suitable dispersant must be found to ensure the suspension remains stable. In this program, an initial particle and dispersant screening process was developed and reduced to a standard procedure with evaluation criteria. Multiple dispersants and particles were assessed as dilute suspensions, and the most promising dispersant compounds and concentrations identified and used for further investigation with higher particle loading fractions. Although the manufacturers' advertised specifications fell within the size criterion for forming a stable suspension, all commercially available nano-sized aluminum particles examined were found to be unsuitable in the as-delivered state. A high fraction of the particles were determined to be in the form of undispersable permanent agglomerates made up of many primary particles, represented as an Average Agglomeration Number (AAN) significantly greater than 10. After removal of the oversized agglomerates through settling and filtration, only an unacceptably small percentage of material remained in the dispersed state (often >90% loss). Therefore, initial steps were made in assessing and testing additional processing procedures (i.e., filtering, milling, etc.) that would be necessary to generate a suitable long-term stable colloidal suspension.

INTRODUCTION

Micrometer-scale combustible metal particles have been traditionally added to solid propellants as performance enhancers and combustion stabilizers at levels of tens of percent of mass fraction.¹ Addition of combustible particles to liquid propulsion fuels (e.g., JP-8 or RP-2) also has the potential to significantly enhance performance, especially in terms of increased energy density. However, unlike in solid propellants where the particles are stabilized in a fixed binder, a liquid fuel provides a mobile phase through which the particles can move, allowing settling due to gravitational forces (or other acceleration), and agglomeration. Previously, this issue has been addressed by using high loading densities or gelling agents to greatly increase the liquid viscosity, thereby reducing the particle mobility. Since the extreme modification of physical and transport properties makes the resulting fuel mixture unsuitable for use in existing systems, consideration of changes in pumping requirements, spray breakup, heat transfer, ignitability, etc. must be taken into account.

Ideally, one could add a significant (in terms of performance enhancement) fraction of combustible particles to a liquid fuel, while retaining compatibility with existing handling and combustion

Distribution A: Approved for public release; distribution is unlimited.

systems (or at least require minimal modifications). Thermochemical calculations (using the NASA-CEA code² with shifting equilibrium and perfect expansion from a chamber pressure of 1,000 psia to atmosphere at sea-level) show that even 5 weight percent of a combustible metal in a liquid fuel (e.g., RP-1) can provide notable benefits to a liquid oxygen (LOX)/kerosene rocket propulsion system in terms of density-specific impulse and shift in optimum oxidizer/fuel (O/F) mixture ratio to more balanced tank sizes. A set of plots displaying calculated values for aluminum, titanium, and tungsten additives are shown in Figure 1 to illustrate the potential benefits. When used in stable dispersions of small additive percentages, only limited physical changes to existing combustion systems may be necessary. In particular, these enhanced fuels can offer increased performance in volume-limited propulsion systems. However, to date, development in liquid propulsion fuels of low, stable concentrations of nano-sized particles which do not significantly alter the flow characteristics of the fuel has been very limited.

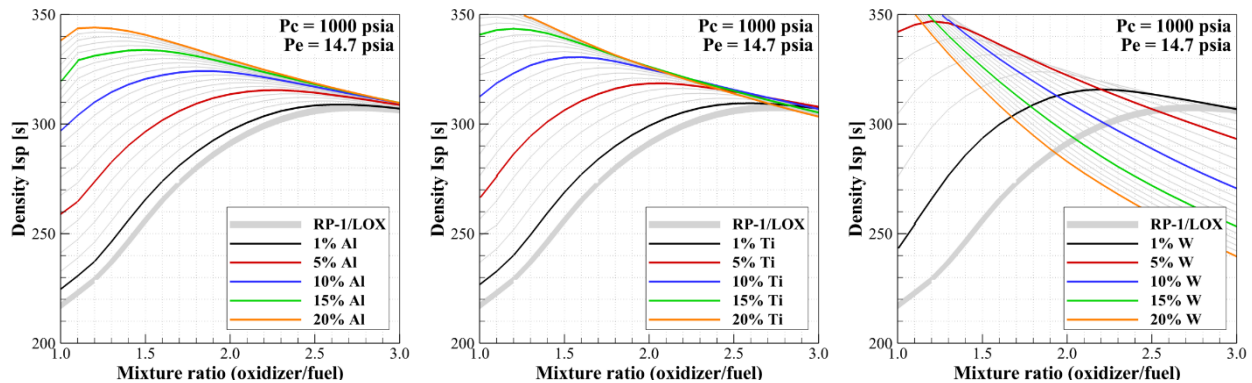


Figure 1. Calculated Density- I_{sp} (using average propellant specific gravity) for an RP-1/LOX boost propulsion system as a function of additive weight percent and oxidizer/fuel mixture ratio for aluminum, titanium, and tungsten.

With recent improvements in the production and affordability of a wide variety of nano-sized particles, advances in colloidal science of nano-sized metal particle/liquid suspensions, the development of practical enhanced nano-fluid fuels can now be considered. Study and ultimately implementation of these nano-fluid fuels in aerospace propulsion systems offers the opportunity for theoretically predicted performance increases to be realized.

OBJECTIVES

Work reported in this paper was performed as part of a Small Business Innovative Research (SBIR) Phase I program that included ignition and combustion studies of certain nanofuel formulations. The focus of this paper is the fundamental material science aspects related to the examination and optimization of particle suspension characteristics. Therefore, the objectives to be addressed here are associated with that portion of the study:

- Determine and apply appropriate particle selection criteria;
- Develop screening techniques to quickly assess as-delivered commercial particle suitability;
- Find effective particle dispersants for use with RP-2
- Perform an optimization study for the required amount of dispersant and processing technique;
- Assess particle dispersions for combustion system applications; and
- Provide recommendations for future process and technique improvements.

BACKGROUND

In recent studies, a number of researchers have generated mixtures of nanopowders in non-aqueous liquid fuels to assess fluid behavior and ignition/combustion characteristics, but these mixtures were neither formulated nor evaluated for long-term stability. The physical characteristics of a wide variety of nano-sized particles, in some cases commercially available, as considered for propulsion

applications were tabulated by Risha et al.³ The fluid behavior and ignition of several RP-1 and nano-Al (Alex[®]) gelled propellants was investigated by Tepper and Kaledin.⁴ Jones et al.⁵ measured the heat of combustion of mixtures of nano-sized aluminum (n-Al) and nano-sized aluminum oxide (n-Al₂O₃) in ethanol with a bomb calorimeter. Stable suspensions of n-Al in ethanol up to 10% volume loading and 5% for n-Al₂O₃ were observed. Gan and Qiao⁶ investigated the burning characteristics of 10 wt% (~3% by volume) n-Al (80 nm) and micron-sized Al (5 μm) in n-decane and ethanol, both with and without a surfactant (sorbitan oleate at 2.5 wt%). They also compared the suspension characteristics of the two sizes of aluminum, showing that mixtures with n-Al stayed in suspension longer. Noting that prevention of the flocculation of n-Al is paramount for application to systems beyond controlled laboratory experimentation. Gan et al.⁷ also examined the combustion of droplets of n-decane and ethanol containing 5 to 20 wt% boron (80 nm) and iron (25 nm) nano-sized particles in the same experimental setup⁶ with 0.5 wt% of surfactant for decane mixtures and no surfactant for mixtures in ethanol. Sabourin et al. examined the burning rates of nitromethane (a monopropellant) solutions with both n-Al and fumed silica⁸ and functionalized graphene⁹ in a liquid propellant strand burner.

RESULTS AND DISCUSSION

In this program, an initial particle and dispersant screening process was developed and reduced to a standard procedure with evaluation criteria. A number of dispersants and particles were assessed, and the most promising dispersant concentrations identified for further investigation with higher particle loadings. Since all commercially available particles examined were found to be unsuitable in the as-delivered state, initial steps were made in assessing and testing additional processing procedures (i.e., filtering, milling, etc.) that would be necessary to generate a suitable colloidal suspension.

PARTICLE SELECTION CRITERIA

While a number of materials may be considered for the inclusion in liquid propulsion fuels, the most available/affordable materials with high volumetric heats of oxidation are attractive for commercialization. These include but are not limited to aluminum, boron, boron carbide (B₄C), carbon (graphene), titanium, and tungsten nano-sized particles.

When properly dispersed in a fluid, the predominant forces on particles consist of gravitational (or accelerational) settling and Brownian motion. The accelerational settling is caused by the net body force on the particle due to external acceleration (from gravity and/or other bulk motion of the fluid containing the particles, such as the fuel tank in a boost-phase rocket or a maneuvering aerospace vehicle). Brownian motion is due to collisions with the fluid particles in thermal motion, resulting in random motion related to the fluid temperature and fluid viscosity. For a given period of time, the ratio of particle displacements due to these two types of forces can be compared to determine the dominant effect on the particle motion. Using well-established physical models describing particle motion in fluids and following the analyses of Allen (1990)¹⁰ and Moore & Orr (1973)¹¹, it was found that that particles in the 10's of nanometers are expected to be stable against long-term settling over the entire military range of temperatures for combustion systems using RP-2. That is, the random thermal motion is dominant over bulk particle motion caused by any acceleration vector. As might be expected, particles of less-dense substances (e.g., boron, aluminum, titanium etc.) form stable suspensions at larger sizes [O(100 nm)], while denser materials (e.g., tungsten) are only stable at much smaller particle sizes (<50 nm). The precise size criterion for stability depends on particle density, fluid properties, temperature, and vehicle motion (i.e., acceleration); detailed discussion of this analysis will be provided in an upcoming manuscript.¹² However, these approximate values provide sufficiently detailed size criteria to allow vetting of commercially available particles for suitability.

INITIAL AS-DELIVERED PARTICLE ASSESSMENT

For detailed examination of the particle and agglomeration characteristics and comparison to manufacturer's specifications, small samples of selected as-received particles were examined at high magnification using a field-emission scanning electron microscope (FESEM).¹³ To provide a clear

background, scrap silicon wafer fragments were used as substrates. To prepare for the sample mounting, they were alternated three times between base and acid washes. After rinsing with deionized water and air-drying, the substrates were mounted on the SEM stub bases using conductive carbon tape, and further electrically bonded using a dot of conductive graphite paint at one corner. To dilute the particle number density to an appropriate level for imaging, the particle/fuel mixes were agitated using a vortex mixer for approximately 5 seconds, then one or two drops were placed into 5 mL of cyclohexane (C₆H₁₂). Ten μL of the diluted mixture was pipetted onto the silicon wafer and allowed to dry. No further sample preparation (e.g., sputtering) was performed before placing the samples into the FESEM instrument for examination. Images and analysis of 0.1 vol% mixtures with RP-2 (before dilution in hexane) for certain particles are given below. RP-2 Batch No. YA2921HW10 (as provided from the Air Force Research Lab, Edwards Air Force Base) was used for all dispersion characterization and testing.

US Nano Aluminum Powder (40nm nominal)

Figure 2 shows the qualitative evaluation of the state of agglomeration in the 0.1 vol% mixture by optical microscopy. Obviously, large agglomerates are present in the mixture. FESEM micrographs of a typical agglomerate are shown in Figure 3. For reference, Figure 4 shows the manufacturer-supplied SEM image of this particle type. As can be seen in the right-hand image of Figure 3, the constituent particles are consistent with the manufacturer's 40-nm value. The presence of a small number of single particles or clumps of only a few particles (as seen in the upper left-hand side of both images in Figure 3) provides some indication that the agglomeration may not be permanent, and these 40-nm particles could be dispersed with the use of an additive.

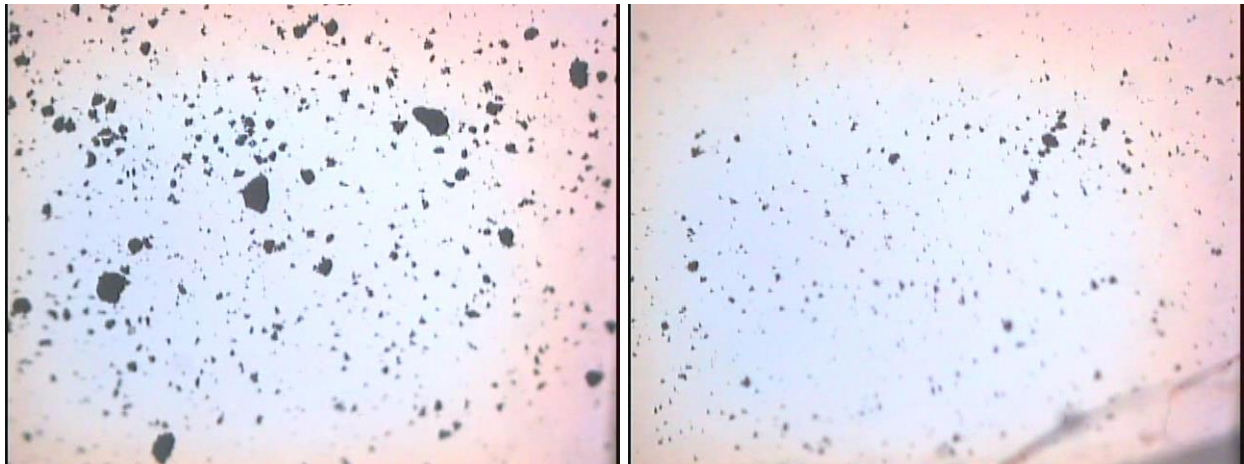


Figure 2. Images of US Nano aluminum (40 nm) from optical microscope using 10x objective lens.

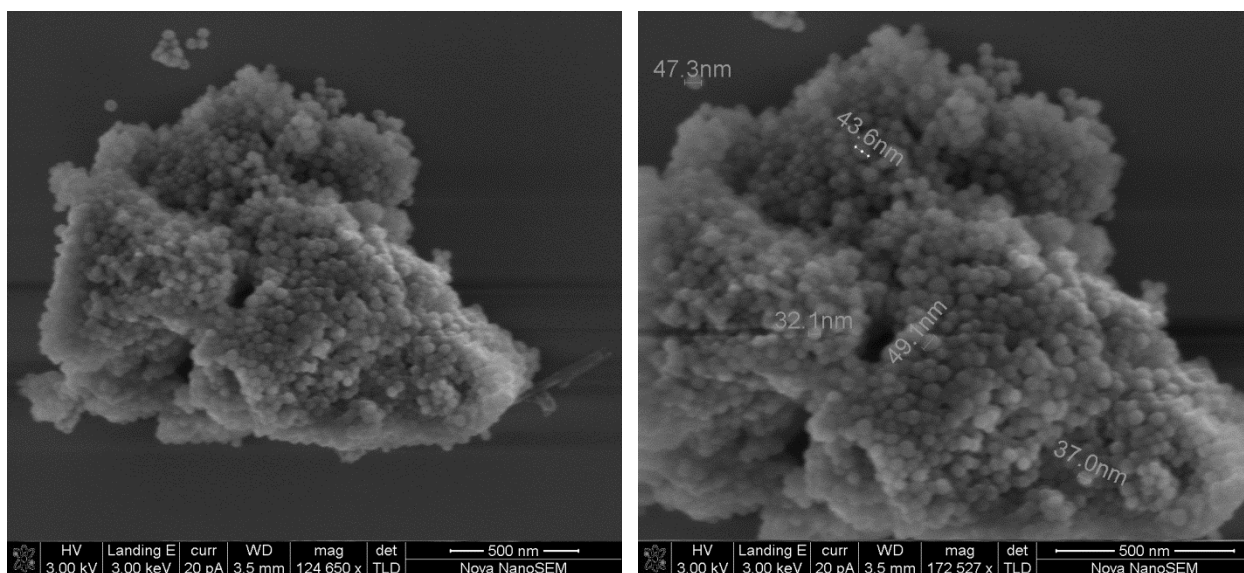


Figure 3. FESEM micrographs of the selected agglomerate of the US Nano aluminum (40 nm) after mixing with RP-2.

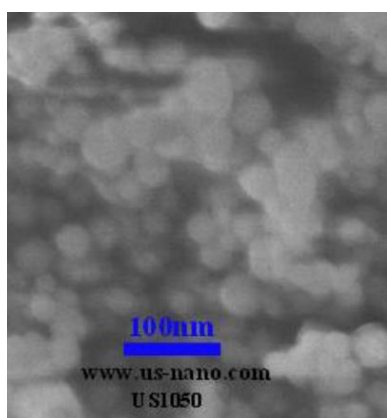


Figure 4. Characteristic manufacturer-supplied SEM micrograph of US-Nano aluminum (40 nm) particles.

Novacentrix Aluminum Powder (80-nm nominal)

Two different lots of 80-nm aluminum powder from Novacentrix were examined. The first, an older lot previously acquired for other studies, exhibited poor wetting in RP-2 and was not considered further. A more recent lot (Batch 090310-2) seemed better in terms of the initial evaluation of wetting, and its dispersion characteristics were therefore further investigated later in the program. Although not explicitly specified by the manufacturer, the behavior of the older lot is indicative of some sort of surface treatment prior to delivery; in fact, the packaging mentioned that it contained carbon (perhaps in the form of a surface passivating agent or pre-added dispersant). The more recent batch only mentions that the packaging contains nitrogen, hopefully implying that no additional surface treatment has been performed. An example image of this material (actually, a micrograph of the same 80-nm grade from the corporate predecessor of Novacentrix, Nanotechnologies) is shown in Figure 5.

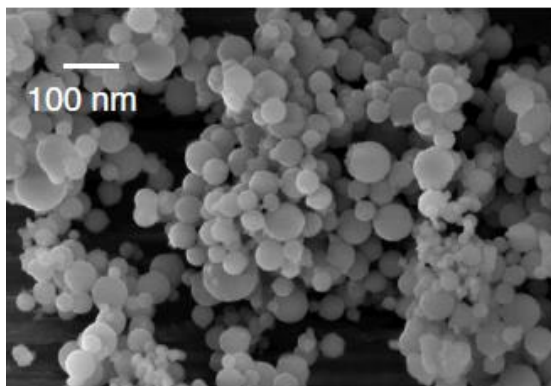


Figure 5. High-resolution SEM micrograph of 80 nm spherical aluminum particles (image taken from Risha, et al.¹⁴ and credited to Mr. Ed Roemer).

SB99 Boron Powder (<150 nm nominal)

Although no longer commercially available, a supply of SB99 boron (SB Boron Corporation) was available on-hand, and used as an example of a nano-scale boron powder. It shows much smaller and more regular structures than the aluminum powders under 10x optical observation (Figure 6). However, the fact of visibility implies that the structures are still much larger than the nanoscale. When diluted for FESEM imaging, smaller-scale individual agglomerates became apparent (seen in Figure 7). At this time, it is not known if they were also present in the initial RP-2 mix, or if the SB99 powder dispersed more effectively in the cyclohexane diluent. Dark-colored “blotches” in the background of the FESEM images are attributed to incomplete and irregular vaporization of the RP-2 components. The observed boron particle agglomerate sizes of hundreds of nanometers to nearly one micrometer are consistent with agglomeration sizes observed by Young, et al.¹⁵ for the same material.

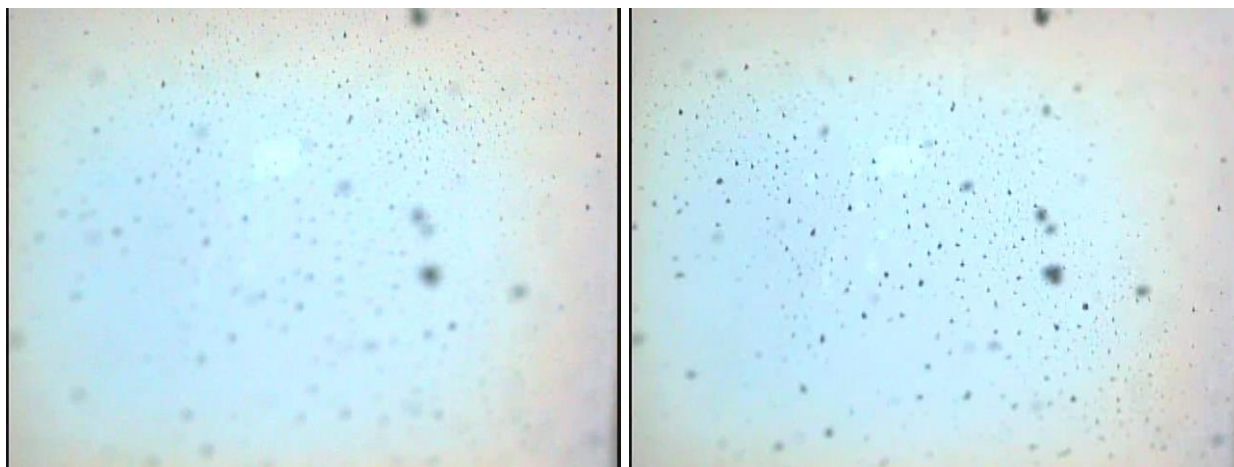


Figure 6. Images of SB99 boron powder (<150 nm) from optical microscope using 10x objective lens.

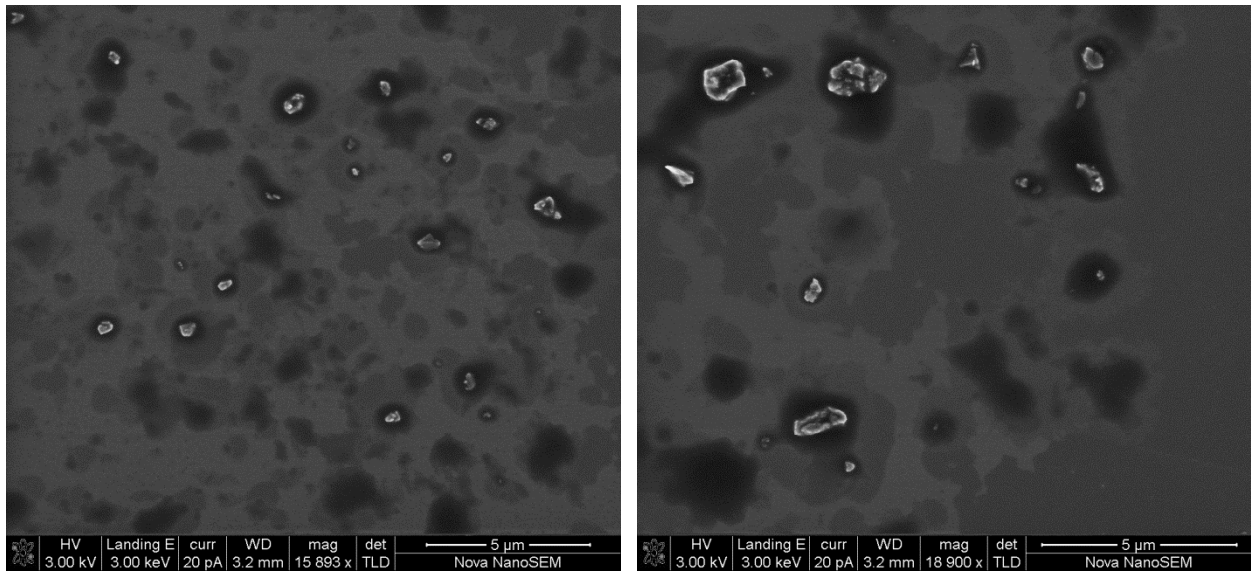


Figure 7. FESEM micrographs of SB99 boron powder (<150 nm) after mixing with RP-2.

US Nano B₄C Powder (45 – 55 nm nominal)

Similar to the other materials discussed above, 10x optical images of the US Nano B₄C powder (Figure 8) show large visible agglomerates. In Figure 9 and Figure 10, FESEM images show that the agglomerates contain multiple nano-sized particles, permanently bridged and fused together. The manufacturer's SEM image also shows a high degree of agglomeration, but the permanent nature is not as evident. Application of a dispersant will not be able to break this physical connection as seen in the FESEM images. Therefore, this type of powder was ruled out for further consideration.

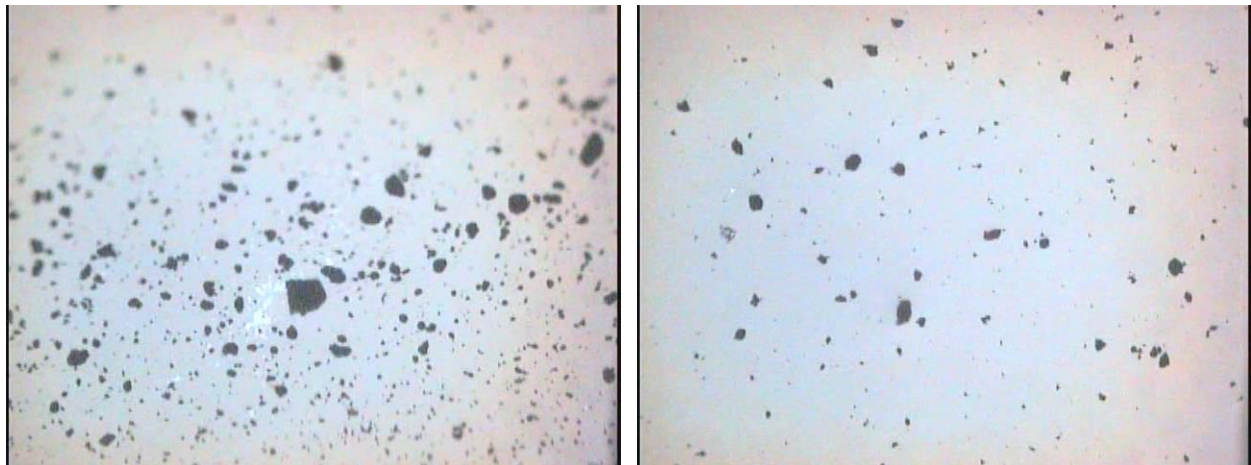


Figure 8. Images of US Nano B₄C powder (45 – 55 nm) from optical microscope using 10x objective lens.

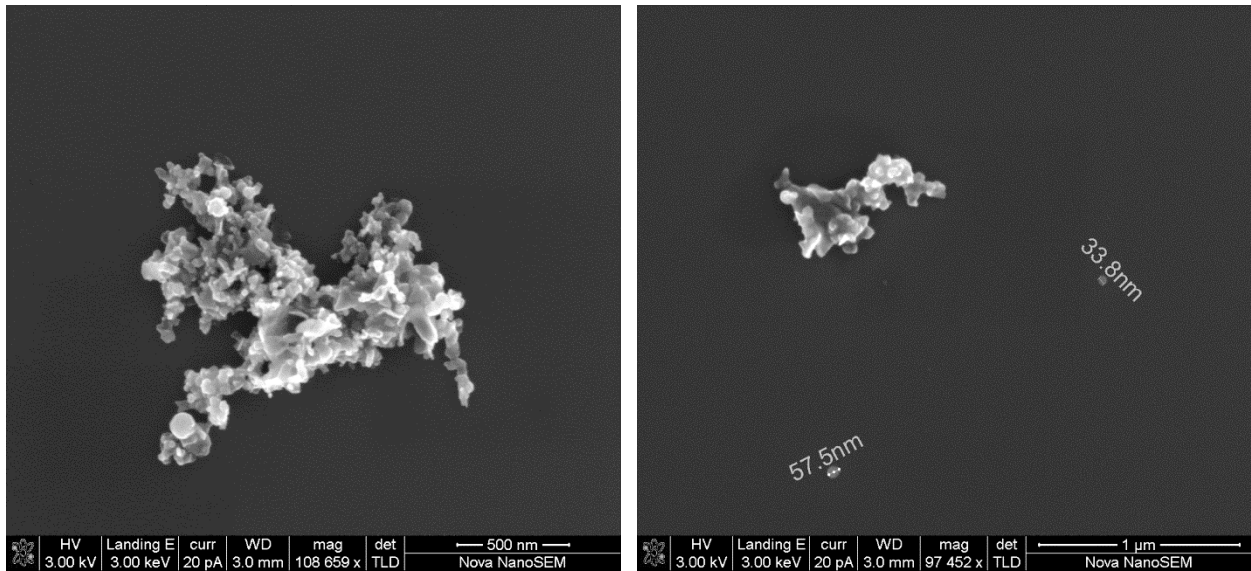


Figure 9. FESEM micrographs of US Nano B₄C powder (45 – 55 nm).

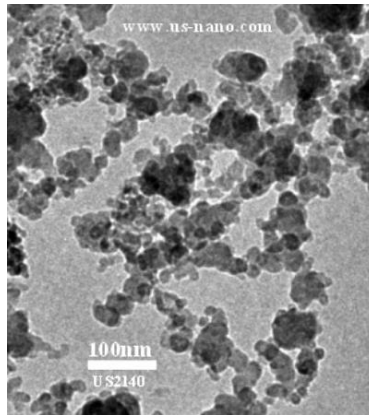


Figure 10. Characteristic manufacturer-supplied SEM micrograph of US-Nano boron carbide particles (45 – 55 nm).

US Nano Iron Powder (25 nm)

The same large-scale agglomeration structures as in the other powders are seen in the 10x optical images for US Nano Fe powder (Figure 11). However, observed behavior in the FESEM images (Figure 12) is very attractive –individual separated nano-scale particles are seen, with nearly no agglomeration behavior. Since the original RP-2/particle mix has been diluted with cyclohexane (and agglomerates were seen in the optical images), this material will still require an effective dispersant, but it is obvious that many of the particles are not permanently agglomerated and can be permanently dispersed with the suitable surface treatment. It is encouraging to obtain this nearly non-agglomerated state, even though the manufacturer’s SEM shows long-chain agglomerates of particles (although under unknown preparation conditions) in Figure 13. The rose-like chunk (on the upper left side of the left image of Figure 12) appears to be a unitary particle, and not an agglomeration of the smaller spherical particles. This is also true for the broken shell-like structure material. The presence of these very different particles may be evidence of contamination or inconsistency in the production process of the nano-Fe material. Due to their much larger sizes, these irregular-shaped particles could be separated out using centrifugal force effect to cause sedimentation.

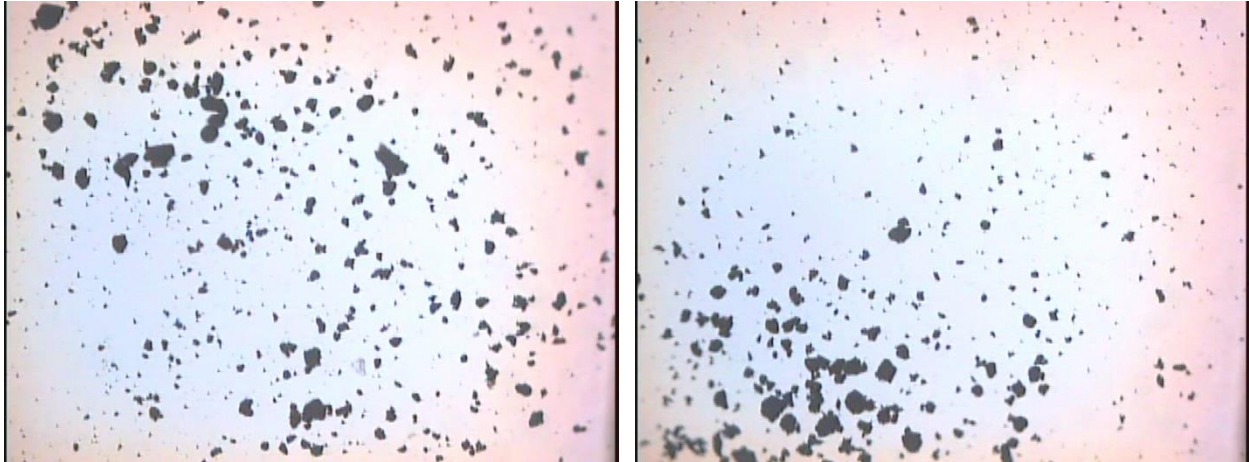


Figure 11. Images of US Nano Fe powder (25 nm) from optical microscope using 10x objective lens.

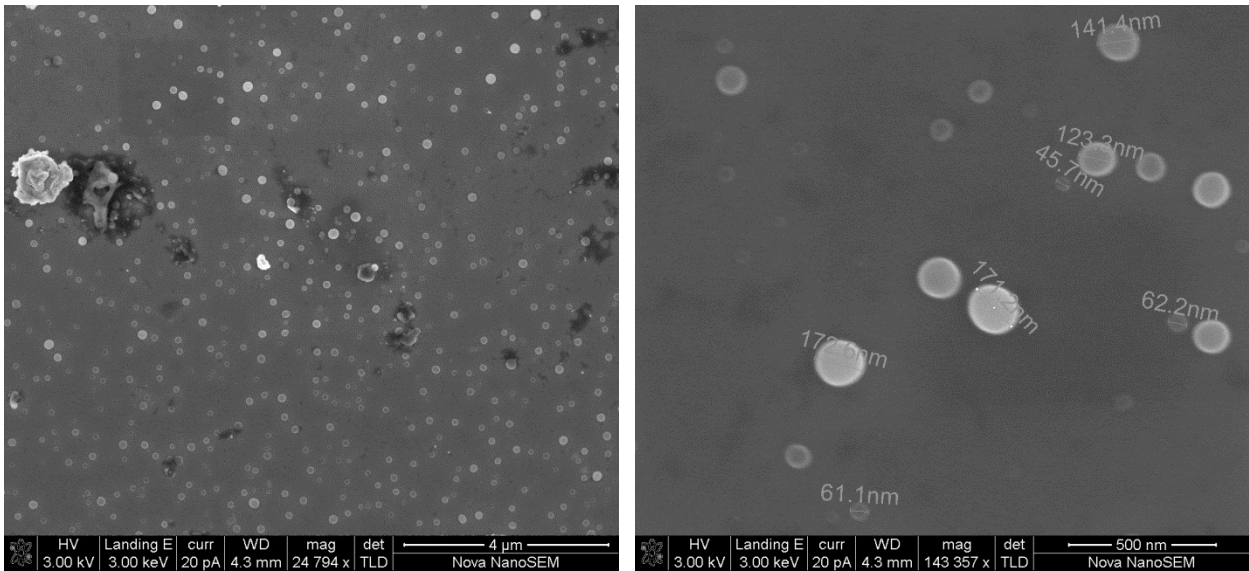


Figure 12. FESEM micrographs of US Nano Fe powder (25 nm).

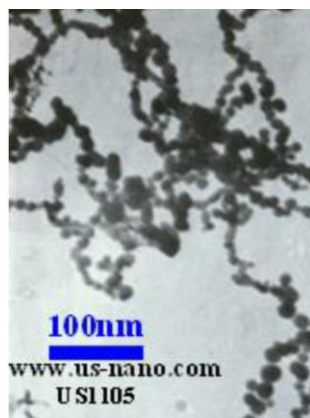


Figure 13. Characteristic manufacturer-supplied SEM micrograph of US-Nano Fe particles (25 nm).

DISPERSANT EVALUATION

Not unexpectedly, all particles examined showed large-scale agglomerations when mixed directly into RP-2 with no surface treatment. Based on a literature search and the authors' experience with similar materials, a list of prospective dispersants for various particle materials was compiled and is given in Table 1. Note that the dispersants are generally expected to interact with the thin oxide coating on the particle surface, and not necessarily with the elemental material. Although not evaluated during this initial search, it is important to identify effective dispersants that require the least amount of additional material to be added to the RP-2/particle mixture and that do not adversely affect the ignition and combustion behavior in propulsion systems.

Table 1. Dispersant materials of interest for various particle types.

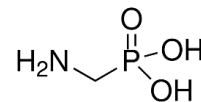
Particle Material	Dispersants Being Evaluated	Comments
Al	Alkyl phosphonic acids with varying chain lengths (methyl, ethyl, butyl, etc.)	Phosphoric acid functional group has been found to bond very well in a monolayer to Al ₂ O ₃ surface ^{16,17}
	(Aminomethyl)phosphonic acid	Available on-hand without ordering
	Oleyl phosphate	If a longer chain is necessary for steric dispersion, this material has the capability.
	Oleic acid	Expected to be effective with Al since all particles will have an Al ₂ O ₃ surface layer.
B	Oleic acid	Demonstrated as both surface oxide inhibitor and dispersant (in hexane and JP-5) ¹⁸
Ti	Oleylamine	Demonstrated to control growth and dispersion of TiO ₂ nanoparticles ¹⁹
	Hexaldehyde	Shown to produce well-dispersed TiO ₂ in an organic phase (e.g., iso-octane) ²⁰
	Titanyl or silane coupling agents	
Fe	Phosphonic acids	Expected to be effective on many metal oxide surfaces.
W	Trioctylphosphine oxide (TOPO) and/or oleic acid	Combination of materials was found to provide effective control of tungsten nanoparticle growth and dispersion ²¹

Ideally, a small amount of dispersant can be added directly to the RP-2 (either before or after particle addition). This assumes some degree of solubility of dispersant in RP-2 to allow transport of dispersant molecules to the particle surface. Even if the dispersant is only slightly soluble in RP-2, it can still be effective since the amount of dispersant needed to generate a molecular monolayer on the particle surface is very small. If the dispersant has no or very low solubility in RP-2, another non-aqueous intermediate solution can be used (e.g., ethanol, dimethyl sulfoxide [DMSO, (CH₃)₂SO], etc.) to apply the dispersant to the particle surface. A non-aqueous solvent is desirable to prevent additional oxidation of the particle surface that could occur by reaction with water. After separation using dry or wet (e.g., centrifuging) methods, the treated particles can be transferred to the RP-2 fluid. Because of the additional complexity, it is preferred not to use this type of method unless totally necessary. Heating of the RP-2 may also be used to temporarily modify the solubility behavior until the dispersant has sufficiently interacted with the particle surfaces.

One of the key parameters for the initial assessment of potential dispersants is the ability of the material to remain soluble in RP-2 over a wide range of concentrations to allow dose-response tests to be conducted on various particles. Low concentrations could be effective, but the time scales might be quite long, so it is desirable to be able to test the dispersant over a wide concentration range. Following from the table of potential dispersants given above, the dispersants that were evaluated include:

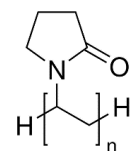
(Aminomethyl)phosphonic acid: $\text{NH}_2\text{CH}_2\text{P}(\text{O})(\text{OH})_2$

This material was considered since the phosphoric acid functional group has been found to bond very well in a monolayer to Al_2O_3 surface. However, it was determined to be **not suitable** since it has very low solubility in RP-2, and therefore sufficient material could not be transported to the particle surfaces in a reasonable time period. In addition, phosphorus-based materials have been considered as fire suppressants (through both chemical and physical effects) that may affect metal combustion,^{22,23} so similar compounds were not further considered.



Polyvinylpyrrolidone (PVP): $(\text{C}_6\text{H}_9\text{NO})_n$ (varying molecular weights available)

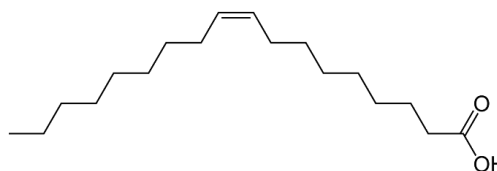
PVP is commonly used as a dispersant for processing of nanoparticles in both aqueous and non-aqueous solvents. It is also available in multiple chain lengths (i.e., molecular weights) that may be useful in minimizing the amount of dispersant needed while still maintaining the suitable effect. However, when added to RP-2 it had limited solubility, exhibiting phase separation with increased concentration and molecular weight at concentrations below the desired values for particle treatment and screening.



Therefore, it is considered **not suitable**.

Oleic Acid: $\text{CH}_3(\text{CH}_2)_7\text{CH}=\text{CH}(\text{CH}_2)_7\text{COOH}$

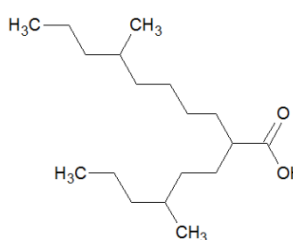
Oleic acid (OA or OAc) has been demonstrated as both a surface oxide inhibitor (for boron) and particle dispersant in non-aqueous solvents (e.g., hexane and JP-5). It is considered **suitable** for further testing since it demonstrated solubility over a wide range of concentrations in RP-2.



During the investigation, two additional candidate dispersants with desirable structural characteristics became available in small quantities suitable for evaluation. These materials, provided by Nissan Chemical Industries Ltd. (and available from Nissan Chemical America Corporation), were Iso-Stearic Acid-N and FO-180, part of their FINEOXCOL[®] line of highly branched saturated fatty alcohols and acids.²⁴

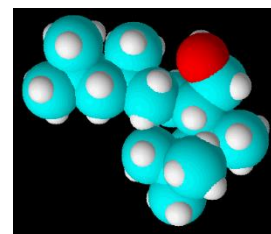
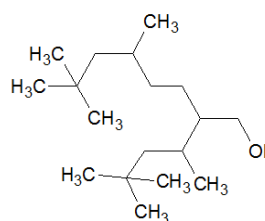
Iso-Stearic Acid-N: $\text{C}_{17}\text{H}_{35}\text{COOH}$

Iso-stearic acid-N (IAc-N). IAc-N is a form of iso-octadecanoic acid, with less branching than iso-stearic acid. The initial boiling point is 320 °C with a decomposition point of 367 °C. It is considered **suitable** for further testing since it demonstrated solubility over a wide range of concentrations in RP-2.



Iso Stearyl Alcohol FO-180: $\text{C}_{18}\text{H}_{37}\text{OH}$

Iso Stearyl Alcohol FO-180 is a highly branched C18 alcohol; further processing can yield derivatives such as isostearyl isostearate. The initial boiling point is 295 °C with a decomposition point of 299 °C. Initial compatibility testing with RP-2 and aluminum particles showed phase separation and large agglomerates, therefore it was considered **not suitable** for use.



PARTICLE DISPERSION SCREENING USING DOSE-RESPONSE STUDIES

Optical Microscopy Observations

It is desirable to use optical microscopy for the initial screening of nanoparticle dispersion characteristics in RP-2, since it is quicker, more accessible, and less expensive than other more “precise” instruments (e.g., SEM, particle sizers, etc.). Because nanopowders in small quantities can be expensive, being able to evaluate the dispersion behavior with small samples is very helpful. Optical microscopy observations are semi-quantitative, but can be very efficient for dosage comparison and trend identification when used as a screening tool for eventual evaluation of dispersant concentration at higher solids loadings. However, this technique requires an experienced/trained observer; as applied to this program, the evaluations are based on familiarity with tens of thousands of optical micrographs viewed by one of the team members. It also assumes similarity in behavior at various dispersant concentrations and solids loading; in other words, poor dispersion at lower solids loading is used as an indication of (expected) poor dispersion at higher solids loading. As long as this relationship holds true, one can eliminate dispersant dosages that have poor dispersion characteristics at low solids loading before moving to more expensive and more labor-intensive larger batches and high solids loading mixes.

The optical screening is used for an initial evaluation with *chemical dispersion only* (i.e., no mechanical processing of particles or fluid beyond minor agitation). This isolates the fundamental action and effectiveness of the dispersant material and particle characteristics from other processing effects. The following procedure was developed and utilized:

1. Make mixture of desired dispersant concentrations in RP-2
 - a. ~8 mL of RP-2 per test vial
 - b. Dose-Response study has varying dispersant concentrations (covering orders of magnitude in concentration)
2. Add nanoparticles to fluid (in glove box, if necessary, for potentially air-reactive materials)
 - a. 0.1 vol% of particles in ~8 mL of RP-2/dispersant solution
3. Agitate using a vortex mixer
4. Equilibrate – allow dispersant interaction with particle surfaces for at least 4 hrs.
5. Briefly agitate, and place droplet on microscope slide
6. Capture images using optical microscope coupled with high-resolution digital single-lens reflex camera (DSLR camera).
 - a. Use a backlit stage on the microscope
 - b. Set to magnification value sufficient to show large agglomerates, but also show reasonable field of view [O(100x)]
 - c. Observe behavior in bulk of fluid as well as near phase boundary

In general, the quality of particle dispersion will vary with the dispersant concentration. Conceptually, the relationship illustrated in Figure 14 can be expected. For simple evaluation, a set of graphical assessment codes has been developed to qualitatively assess the regions seen in the figure:

Obviously Good: 

Worthy of Further Investigation (Marginal): 

Obviously Poor: 

At lower concentrations, the particle surface is insufficiently saturated with the dispersant; since the particle behavior is fundamentally related to the surface chemistry and interactions, this will greatly limit the quality of the dispersion. At increasing dispersant concentrations, the degree of under-saturation becomes less until a region of suitable concentrations is reached. It is expected that there will be a range over which the concentration is sufficient; other factors such as time until equilibrium behavior, desirability of excess dispersant in solution, etc. will determine the optimum concentration. At some even higher level of concentration, the excess dispersant may start to show undesirable behavior such as phase separation or self-assembly (forming structures of combined dispersant molecules).

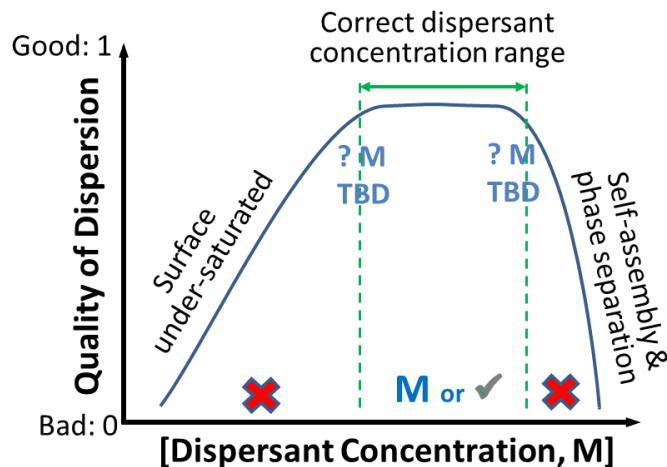


Figure 14. Conceptual illustration of effect of varying dispersant concentration on dispersion quality.

To evaluate the dispersion quality using optical microscopy, the following criteria are applied:

- Apparent sizes of particles (smaller is better)
- Wetting behavior (non-wetting is undesirable)
- Obvious particle clumping and/or agglomeration (presence at any scale is undesirable)
- Particle spacing (evenly spaced particles are better than clustering)
- Bubbles (presence may indicate mixing or wetting issues)
- Phase separation (presence of discrete phase of either particles or dispersants is undesirable)
- Primary particles (presence of non-agglomerated materials is desirable)
- Non-dispersible (“hard”) agglomerates (presence of non-chemically dispersible agglomerated materials is undesirable)

“Obviously Good” means that the mixture has all desirable aspects, and can be used “as-is”. This is not expected to be a common outcome in the initial dispersion screening step. “Worthy of Further Investigation” means there are many desirable aspects, but some bad aspects or behavior that is not clearly good or bad according to the above-mentioned criteria. Further examination can yield supplemental judgment, either “OK” or “X”. Finally, samples performing very badly on a particular criterion or poorly on many can be labeled as “Obviously Poor”. From previous particle dispersion experience, the desirable dispersant concentration range was expected to be 10^{-4} to 10^{-3} M (moles/L). Using standard lab techniques, sets of stock solutions each differing in molarity by an order of magnitude were made; these could then be easily used to generate a wide range of small sample concentrations for evaluating the particle dispersion behavior. Since the dispersant effectiveness is caused by interactions of the dispersant molecules with the particle surface and with one another, molarity is the most relevant concentration measurement to consider.

To illustrate the evaluation technique, optical micrographs corresponding to a selection of the Table 3.4 samples are presented and discussed here. In Figure 15, Images AI-1-5a (no OA or OAc) and AI-1-5b (1.1×10^{-5} M) both show large agglomerates only, and virtually no smaller primary particles; they are therefore rated “obviously poor” as indicated by the red block letter **X**. Image AI-1-5d (3.9×10^{-5} M) shows much better dispersion behavior, with perhaps some primary particles visible (hence, an “M”), but upon further examination, many are still clumped or agglomerated, giving a final rating of “X”. Image AI-1-5e (1.3×10^{-4} M) looks similar in many ways, but the single particles are much more evenly spread throughout the field of view, with very little clumping behavior apparent. While large (~25 μm) possibly as-delivered non-dispersible agglomerates are still visible, this mixture is worthy of further investigation (“OK”). In Image AI-1-5g (1.5×10^{-3} M), there are again many individual small dispersed particles along with the presence of the larger non-dispersible particles (“M”). When the field of view is panned to the liquid-air interface (shown in the inset), there is some collection and clustering of particles, possibly indicating phase separation of the OA and particles due to a very small, but finite amount of water in RP-2. The actual cause is unknown at this time (would require significantly more analysis), but the observed effect

moves the assessment of the mixture to, at best, marginal. Finally, Image Al-1-5h (1.5×10^{-2} M) again shows well-separated particles in the main field, but very undesirable behavior at a different location on the slide. The clumps shown in the inset are likely produced by phase separation of oleic acid at higher concentrations into micellar structures (through self-assembly). The large view is perhaps worthy of further consideration ("M"), but the potential phase separation renders the concentration unsuitable.

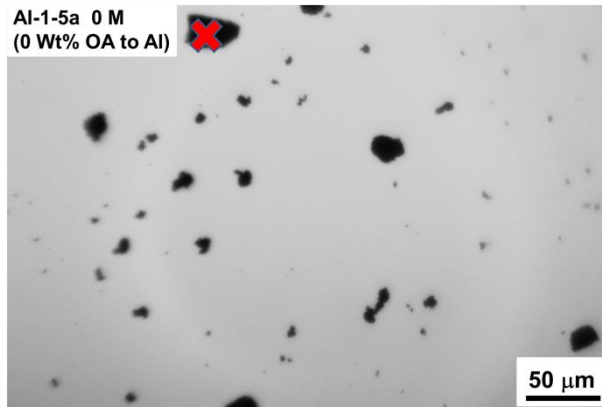


Image of sample Al-1-5a (obviously poor).

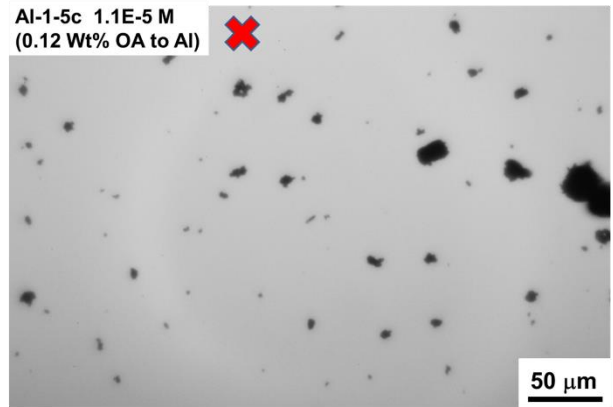


Image of sample Al-1-5c (obviously poor)

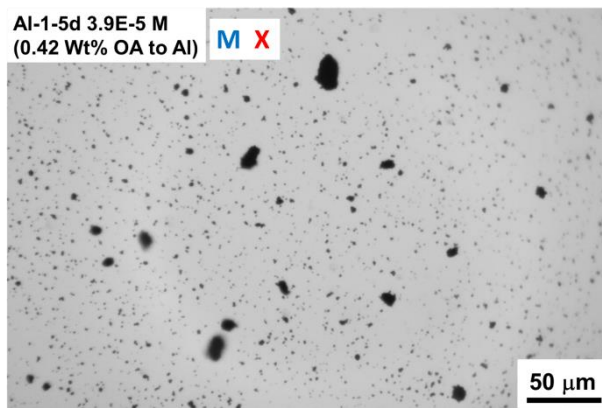


Image of sample Al-1-5d (worthy of further investigation, but most likely poor).

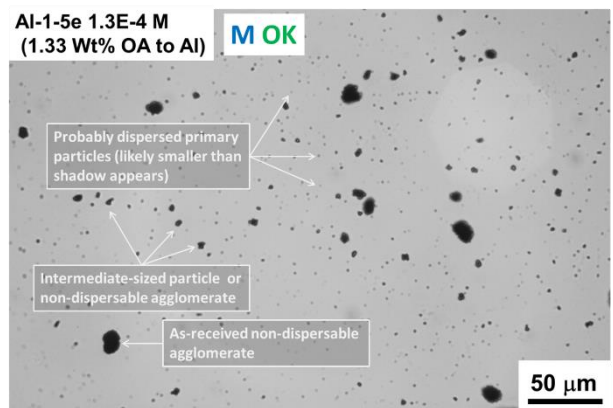


Image of sample Al-1-5e (worthy of further investigation, promising).

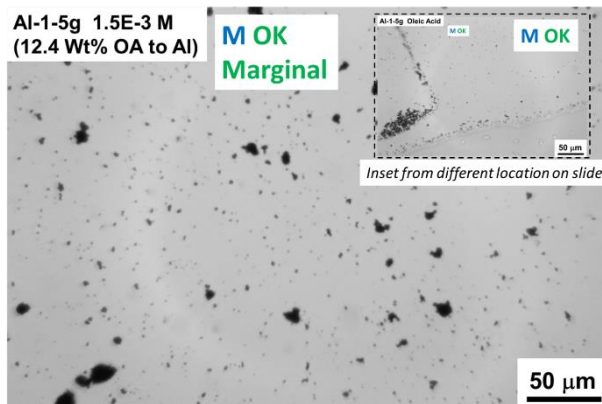


Image of sample Al-1-5g (worthy of further investigation, marginal).

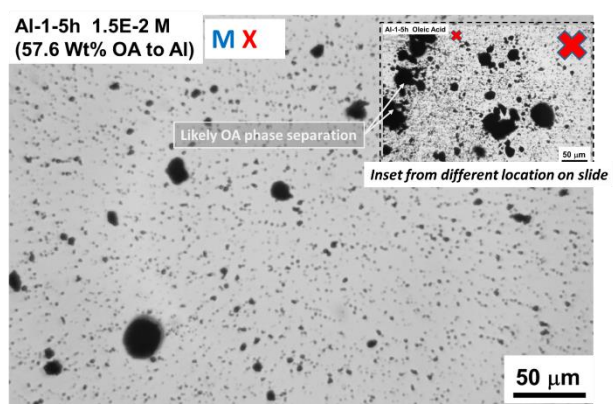


Image of sample Al-1-5h (worthy of further investigation, shows poor behavior at edges)

Figure 15. Optical microscopy images of sample family Al-1-5 with varying dispersant (OA) concentrations.

Recalling the behavior with concentration shown conceptually in Figure 14, the actual concentrations can be mapped onto the abscissa with letters corresponding to the mix concentrations (shown in Figure 16). Using this framework, it can be seen that for this particular particle/dispersant pair in RP-2, the correct dispersant range in fact appears to be between 10^{-4} and 10^{-3} M. This range of values was then used for guidance in scaling the mix to higher particle loadings. Similar testing can establish the desirable dispersant range for other particle types (and other dispersant materials).

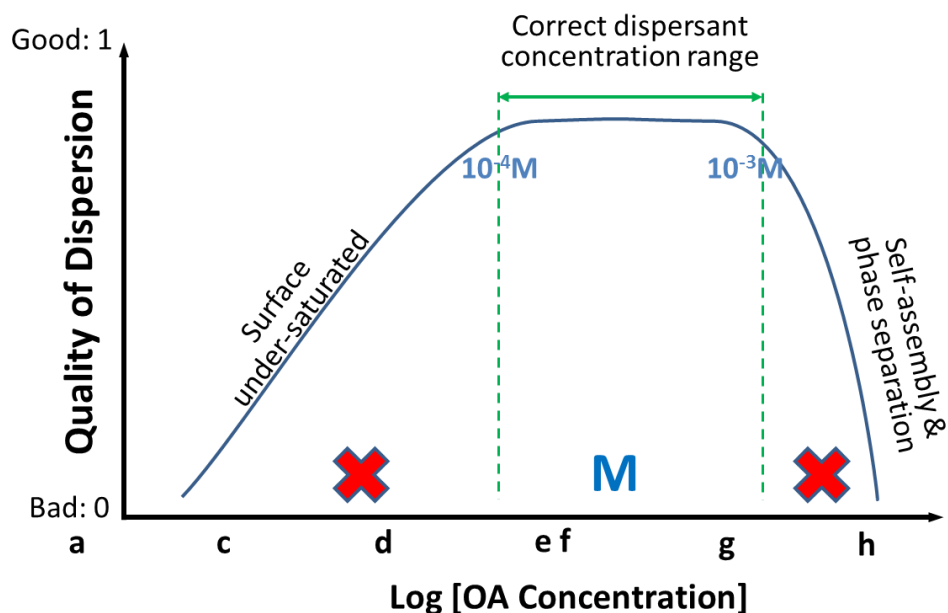


Figure 16. Observed behavior of varying oleic acid concentrations on Al nanoparticle dispersion quality.

As part of the method development and evaluation, at least single-series evaluations were performed for three different types of dispersants and multiple types of particles in RP-2, including two types of Al_2O_3 (as Al surface simulants), three different Al materials, Ti, B_4C , W, B, and Fe.

Gravitational Sedimentation Observations

The optical microscopy observations found that Al nanoparticles dispersed with oleic acid was a combination that showed significant merit. Therefore, a more detailed study using a directly relevant response (i.e., settling behavior) was carried out on the effect of using different concentrations of oleic acid as dispersant for Al nanoparticles. Similar to the procedure described above, mixing was performed by adding desired amounts of oleic acid to RP-2, then adding 10 wt % Al nanoparticles to the RP-2/dispersant solution. The fractions of oleic acid were measured in wt % with relation to the amount of Al nanoparticles added.

Initially, 2 g of RP-2 was added to a 10-mL screw top flasks closed with a PTFE-lined cap. Different amounts of oleic acid were then added to the RP-2 in quantities of 0, 10, 20, 40, 60, and 80 wt % with respect to the amount of U. S. Nano Al (10 wt% of the total) to be added. After initial agitation using a vortex mixer, the vials were allowed to stand undisturbed. Pictures were then taken at $t = 0, 1, 4, 6,$ and 72 hours elapsed time to characterize settling characteristics of the particles in the suspensions. The sediment level was recorded as particles came to rest at the bottom of the vessel. Lower sediment height could indicate two things, better packing density due to more well dispersed particles and/or less particles falling out of the suspension, which also would indicate better colloidal stability.

Shortly after the initial settling study procedure was developed with OA (OAc), two new dispersants (Iso-stearic Acid-N and FO-180 as described earlier) were made available for testing. Using

the established screening procedure, FO-180 was immediately disregarded as a useful dispersant due to the phase separation it exhibited when mixed with the RP-2. In the interests of a direct comparison, the IAc-N was immediately evaluated using the sedimentation testing procedure. Eight grams of RP-2 were used with IAc-N dispersant in the amounts of 10, 25, 50, 75, and 100 wt % with relation to the Al mass. Larger sample sizes were considered than in the earlier sedimentation tests (i.e., 8 g vs. 2 g of RP-2) to allow for the possibility of filtering (described in the next subsection) to remove large undesirable agglomerates. IAc-N was found to have the best results between 30 and 70 wt% with respect to Al. This was determined by a sedimentation study through time lapse photography of vials of suspensions over a range of 10 hours. To provide a direct comparison, OAc was tested again in the same manner and it was found that the most effective dispersant concentrations were between 10 and 40 wt % with respect to Al (consistent with the initial evaluation).

A similar study was carried out with the more recent batch of 80-nm Al particles from Novacentrix. Initial concentrations tested were 10, 20, 30, 40, 50, 75, and 100 wt%. Due to time constraints, only OAc was used as a dispersant with the Novacentrix Al as it had appeared to yield higher-quality suspensions with the U.S. Nano Al powder. For the Novacentrix material, the best results seemed to be between 10 and 40 wt % OAc with respect to the Al. After these suspensions were left overnight (approx. 12 hr), upon visible inspection samples with dispersant concentrations in this range had the least amount of sediment at the bottom of the vials and the highest concentration of suspended particles.

Effect of Filtration

From the sedimentation study, it became clear that a significant portion of the particles, even when well-dispersed, were in the form of undesirably large permanent agglomerates that would not remain suspended over time periods (and acceleration loadings) of interest. Focus was then turned to the effects of filtration on suspension stability. If the larger agglomerates could be removed through filtration, it was expected that more stable dispersions would result. Settling calculations (briefly discussed earlier as one of the particle selection criteria) showed that aluminum particles below 1 μm should exhibit some degree of long-term suspension stability, with a desirable upper size limit of <200 nanometers providing essentially permanent stability for the anticipated storage and usage environment.

To test the filtration procedure with the small samples, syringe filters were first used. The syringe filters were Acrodisc® 25-mm syringe filters with 1- μm glass fiber membranes (Pall Life Sciences²⁵). These allowed small volumes to be filtered by hand, using only a syringe to provide the necessary pressure to force the suspension through the filter. It was found that filtering suspensions through the 1- μm filters lengthened the stability lifetime (according to the sedimentation observations) from hours to several days. However, it was found that large amounts of Al particles were being removed from the suspensions, indicating that a large percentage of oversized particles were present and/or the filter media was loading/clogging and retaining even small particles that should pass through the pores. An attempt was made to quantify the amount lost by weighing the filter before filtration, then again after drying. However, it was found that the mass change of the filters was greater than that of the total of the added Al. This indicated that there were other substances remaining in the filter with the Al particles, most likely the less-volatile portions of the RP-2.

Although the actual solids content could not be easily determined, it was nevertheless deemed valuable to assess the stability of the suspensions filtered with the syringe filters. Particle size distributions were found for suspensions made using the 40-nm U. S. Nano Al particles in RP-2, and varying concentrations of the OAc and IAc-N dispersants. Particle size was determined using a Horiba CAPA-700 Particle Size Distribution Analyzer at 5,000 RPM. The centrifuge feature of the CAPA-700 was used to reduce the measurement time of this sedimentation-style analyzer to a reasonable time (<1 hr). Since the objective of this overall study is to develop suspensions that are unconditionally stable, the standard gravitational sedimentation (i.e., 1 g) mode was unsuitable and much higher accelerations had to be applied to force the nano-sized particles to settle in a reasonable time.

The particle size distribution results for these two types of dispersants (IAc-N and OAc) are shown in Figure 17 and Figure 18, respectively. The graphs of particle size distribution suggest that the

particle sizes, or rather agglomerate sizes, are multimodal. The spikes near one micron indicate that there may be a large population of agglomerates with sizes near and slightly above 1 micrometer. Also, the data show that there are very few primary particles in suspension (indicated by a very small fraction of the particles in the “bin” that contains the cited primary particle size of 40 nm). A clear shift in the distributions can be seen with increasing dispersant content; the “large” (1 μm and/or larger) particle frequency drops off significantly, while the proportion of 0.1 to 0.5 μm particles increases greatly. Suspensions were also made using Novacentrix 80-nm Al particles (new batch) with OAc, and filtered as described above. The results for this material are depicted in Figure 19. For this material/dispersant combination, the qualitative shift in particle size distribution with increasing dispersant is not nearly as apparent.

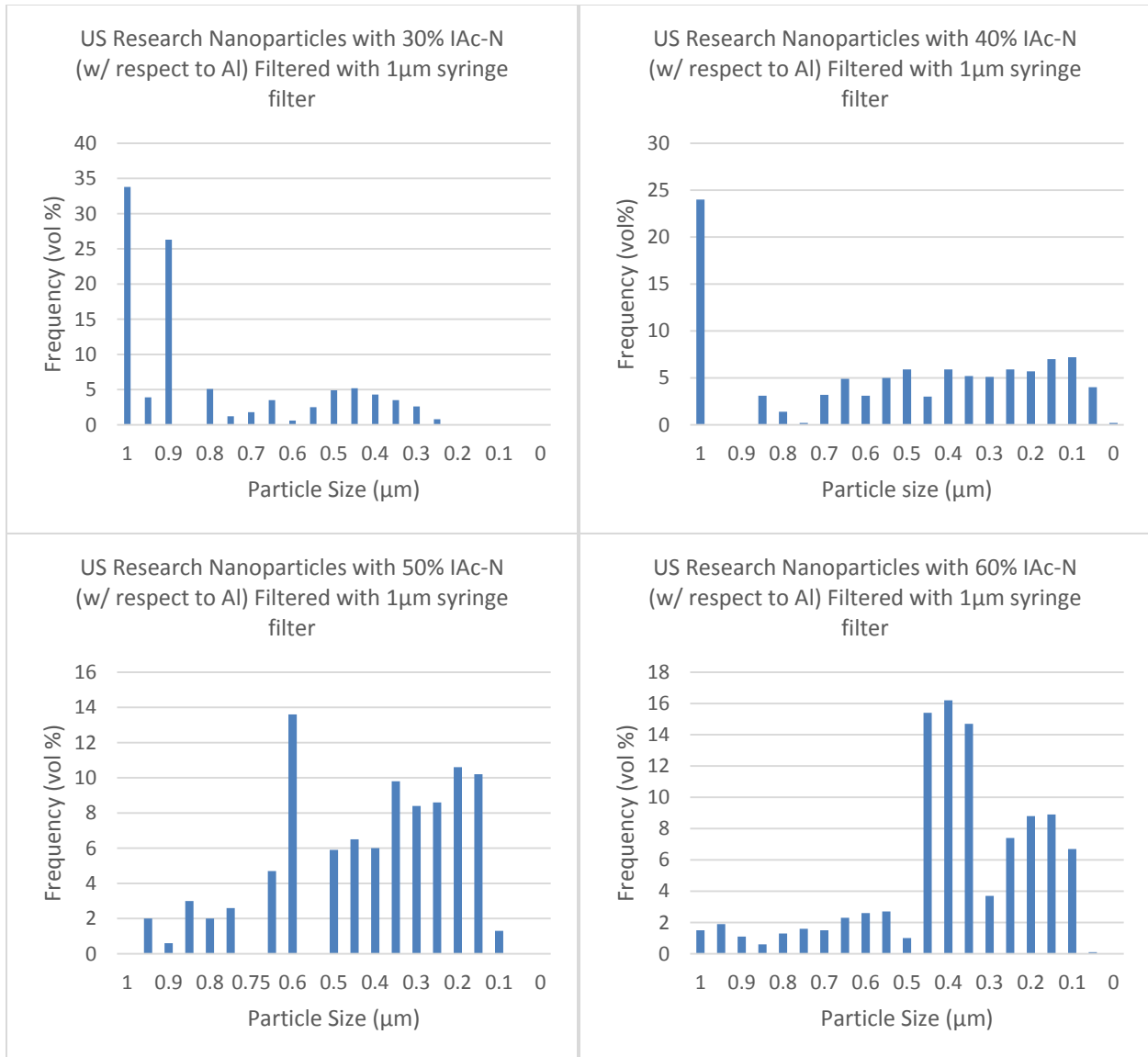


Figure 17. Bar graphs of particle size distributions of U. S. Nano Al suspensions in RP-2 with various concentrations of Iso-stearic Acid-N (IAc-N)

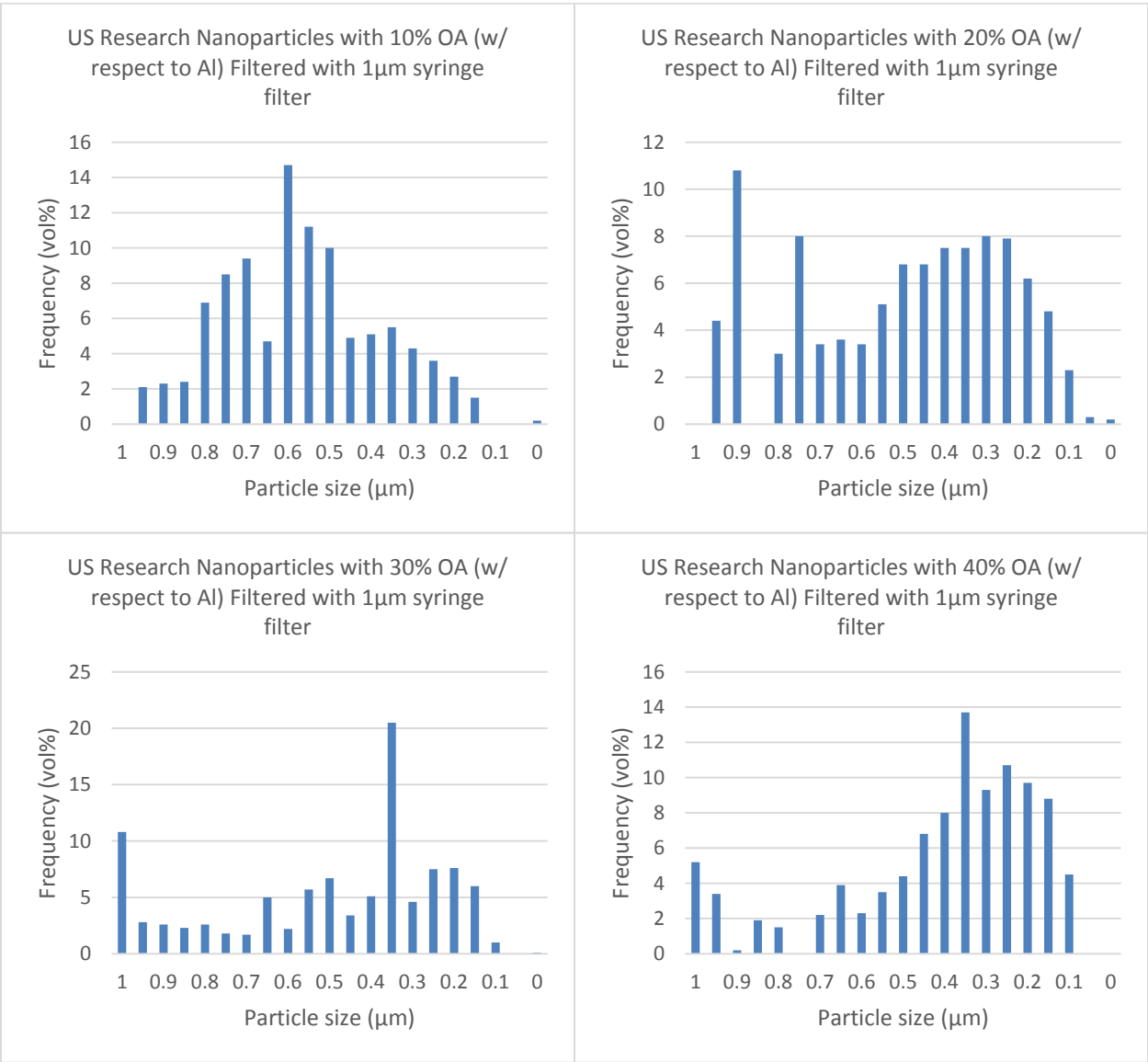


Figure 18. Bar graphs of particle size distributions of U. S. Nano Al suspensions in RP-2 with various concentrations of oleic acid (OA or OAc)

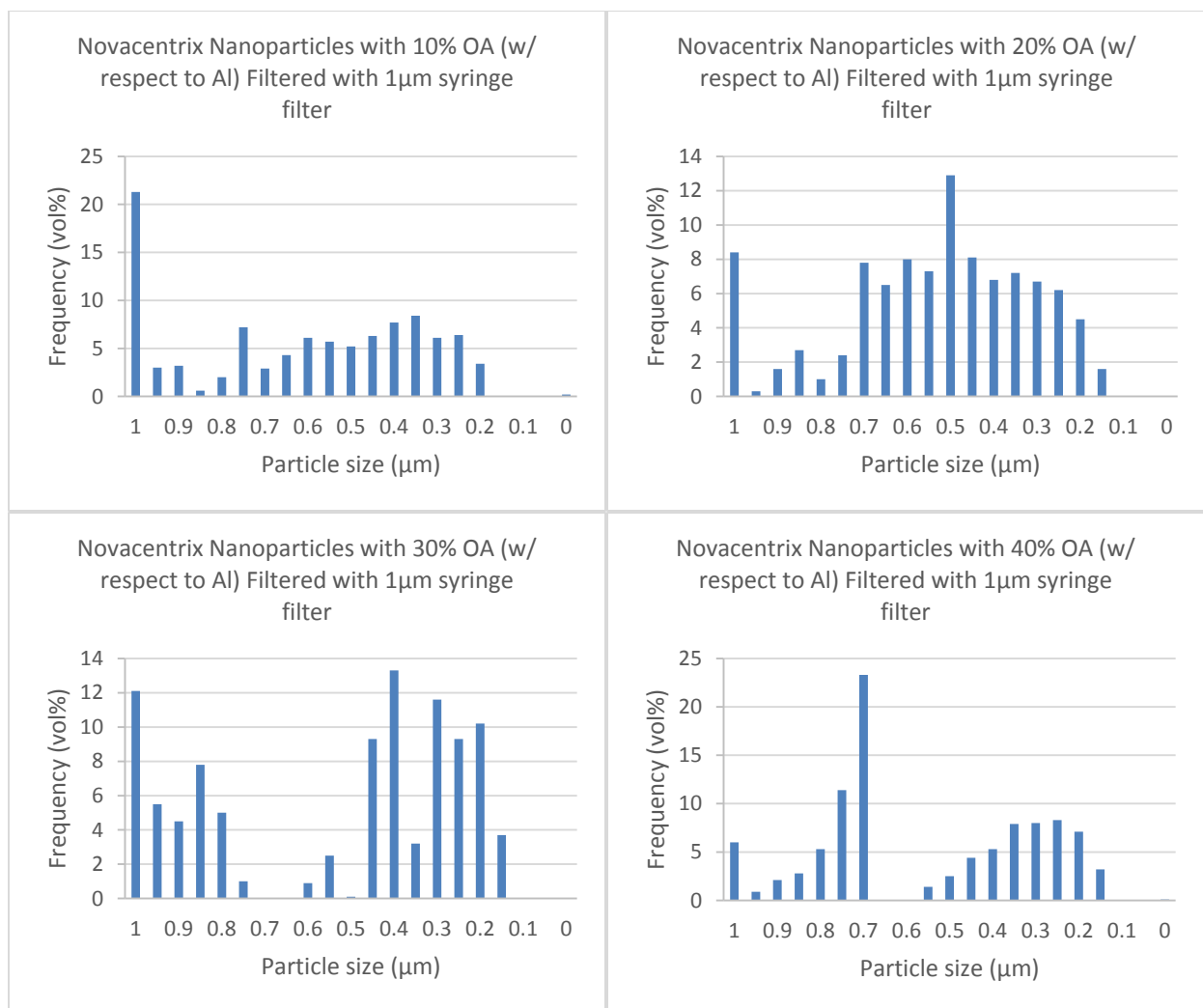


Figure 19. Bar graphs of particle size distributions of Novacentrix AI suspensions in RP-2 with various concentrations of oleic acid (OA or OAc).

From the particle size distributions, average particle diameters were calculated, and are listed in Table 2. From the distribution shapes and average particle sizes, it appears that within the “window” of dispersant concentrations tested (i.e., 10 to 40 wt%), the higher concentrations generally performed better. However, there are enough irregularities in the data that further investigation is warranted before settling on a specific desirable dispersant concentration.

Table 2. Calculated average particle diameters for a different particle/dispersant systems with a range of dispersant amounts.

Dispersant Amount →	Average Particle Diameters [nm]			
	10 wt%	20 wt%	30 wt%	40 wt%
↓ Particle/Dispersant Type				
US Nano 40nm / OA	600	490	430	370
US Nano 40nm / IAc-N	930	510	410	400
Novacentrix 80nm / OA	600	530	440	630

Although some of the filtered materials examined did show stability on the time scales of hours or days, to provide a truly long-term stable suspension over all potential environmental and operational

conditions, all particles should fall below the size criterion. Another filtering step could be performed to remove particles larger than this dimension, but based on the measured distributions of the commercial particles examined, an unacceptably small fraction of material would remain.

COMMERCIAL PARTICLE QUALITY ASSESSMENT

Density and Active Content of As-delivered Particles

Multiple methods can be used to determine the “active” (i.e., un-oxidized) content of the nanopowder materials of interest. These include wet-chemistry, high-temperature thermogravimetric analysis (TGA), and calculation based on particle density. For this Phase I study, the density technique was utilized since it required the least resources (in terms of lab equipment and instrumentation). For the density measurements, a special 25-mL specific gravity bottle (VWR Catalog No. 16629-009) was used. This pycnometer is designed for determining the specific gravity of volatile liquids. The procedure used was based on the ASTM technique for determining density of pigments in solvents (ASTM D153-84); it was modified to suit the available equipment and apparatus, but retained essential steps such as temperature-conditioning the fluid in the pycnometer bottle for accurate and repeatable fluid density determination and subjecting the particle suspension to vacuum to remove any air that may have been trapped at the particle surface. All measurements were made at 20 °C, provided by partially immersing the pycnometer in a Forma Scientific Model 2095 circulator bath. The following steps were taken:

1. Mass of neat fluid (RP-2) to fill bottle at 20 °C was measured;
2. True filled volume of pycnometer bottle calculated from known mass and fluid density (from Outcalt, Laesecke, & Brumbeck (2009)²⁶);
3. Known quantity of nanopowder sample added to RP-2 liquid;
4. Mass of mixture in bottle determined;
5. Using known mass of particles, mass of the RP-2 portion was found, and volume of the RP-2 portion calculated;
6. Knowing total filled pycnometer volume, volume of particle moiety was found;
7. Particle density can be found using the known mass of particle additive.

For the U.S. Nano 40-nm aluminum particles, the technique was applied as follows:

Step 1: mass of RP2 with no Al (m_{RP2}) = 19.9564 g

Step 2: RP-2 fluid (and therefore pycnometer volume) calculated using $\rho_{RP2} = 0.80459 \text{ g/cm}^3$ at 20°C.

$$V_{pyc} = V_{RP2} = \frac{m_{RP2}}{\rho_{RP2}} = \frac{19.9564 \text{ g}}{0.80459 \text{ g/cm}^3} = 24.8032 \text{ cm}^3$$

Step 3: mass of Al added to RP-2 = 1.1676 g

Step 4: After temperature-conditioning and filling mixture into bottle, mass of RP-2 + Al mixture = 20.8362 g

Step 5: mass of RP-2 portion of the mixture (m'_{RP2}) = 20.8362 - 1.1676 = 19.6686 g. Volume filled by this RP-2 portion of the mix is:

$$V'_{RP2} = \frac{m'_{RP2}}{\rho_{RP2}} = \frac{19.6686 \text{ g}}{0.80459 \text{ g/cm}^3} = 24.4455 \text{ cm}^3$$

Step 6: The volume filled by the particles can then be found by the difference between the known total pycnometer volume and the determined RP-2 volume:

$$V_{Al} = V_{pyc} - V'_{RP2} = 24.8032 \text{ cm}^3 - 24.4455 \text{ cm}^3 = 0.3577 \text{ cm}^3$$

Step 7: The particle density can be found from the measured particle mass and determined particle volume:

$$\rho_{Al} = \frac{m_{Al}}{V_{Al}} = \frac{1.1676 \text{ g}}{0.3577 \text{ cm}^3} = 3.2642 \text{ g/cm}^3$$

Similarly, the density for the newer Novacentrix 80-nm material was found to be 2.8621 g/cm³. Since the density for pure aluminum (~2.7 g/cm³) is much less than that of aluminum oxide (~3.95 g/cm³), the Novacentrix material has a significantly higher content of active aluminum, and is therefore expected to release more energy when burned.

Average Agglomeration Number

Average Agglomeration Number (AAN) is a metric developed by Adair²⁷ that uses cubes of diameters instead of the diameters themselves to compare the sizes of actual agglomerates and primary particles. As a result, it compares volumes. AAN is effectively a description of how many primary particles there are, in total, per agglomerate. An AAN is considered good if it is between 1 and 10 (implying a relatively small number of primary particles make up the actual agglomerate particles; 1 would represent totally non-agglomerated primary particles), and poor at higher values. AAN can be defined by the following equation:

$$AAN = \frac{(ESD_{CAPA(V)})^3}{(ESD_{BET(V)})^3} * \phi \quad (1)$$

where ESD is the volume-based “equivalent spherical diameter” as determined by various techniques. $ESD_{CAPA(V)}$ is the average diameter as determined from the particle sizing using the sedimentation technique as implemented in the Horiba CAPA-700 (which was readily available for use in this work); this sort of “envelope” size is also often obtained using the dynamic light scattering (DLS) technique. The denominator of Eq. (1) is the equivalent spherical diameter as determined using a surface area measurement, in this case using the Brunauer–Emmett–Teller (BET) theory (based on surface adsorption of gas). By adsorbing nitrogen to clean surfaces under controlled conditions it can be assumed that the molecules will adsorb in a monolayer. This assumption can be used to find the total surface area and specific surface area (SA/mass). This size distribution is based on number and skews the data to show smaller sized particles more prominently than larger particles. Finally, ϕ is a packing fraction of the particles in the agglomerate; assuming random close packed spheres, $\phi = 0.64$.

The characteristic property determined by the BET analysis is actually specific surface area (SSA) in [m²/g]. The ESD is found from the SSA by:

$$ESD_{by(\#)} = \frac{6}{SSA * \rho} \quad (2)$$

using the actual particle density (as determined with pycnometry in the previous subsection). Equation (3) gives the conversion from average particle size by number distribution to average particle size by volume distribution. This is necessary because particle distribution by volume emphasizes larger particles where distribution by number emphasizes smaller particles. If the two different distribution types were used to calculate AAN then the numbers would not be correct because of these shifts. The ESD can be transformed from number-weighted value to a volume-weighted one using an equation given in Allen (1997).²⁸

$$ESD_{by(V)} = 10^{\log(ESD_{by(\#)}) + \frac{4.6}{s_w}} \quad (3)$$

where $s_w=4$ for commercial powders.

Results of AAN calculations for both U.S. Nano and Novacentrix aluminum particles processed in RP-2, and U.S. Nano aluminum particles processed in cyclohexane are shown in Table 3. The relatively high AAN values found for all particles and processing techniques indicate the fundamental unsuitability of the commercial particles as delivered. They all show significant agglomeration, and an initial effort at pre-processing in cyclohexane yielded significantly worse dispersion than direct addition to RP-2. In terms of consistency between the manufacturers’ cited specifications and actual measured parameters, the primary particle size provided by Novacentrix (80nm) is much closer to the measured value of ~84 nm (via BET) than that of U.S. Nano (40 nm specified vs. ~91 nm measured). The U. S. Nano Al material also had some large “chunks” (perhaps hundreds of microns) found in the powder, while the Novacentrix material appeared much more consistent and uniform. Of course, the chunks could be settled or filtered out easily, but they may be indicative of looser standards in the material production and packaging processes.

Table 3. AAN determination for two different types of aluminum nanoparticles using different processing procedures.

Particle Type	Density [g/cc]	$ESD_{CAPA(V)}$ [nm]	SSA (BET) [m ² /g]	$ESD_{BET(\#)}$ [nm]	$ESD_{BET(V)}$ [nm]	AAN
U.S. Nano 40nm (RP-2/OA)	3.2642	470	20.23	90.867	176.16	19.0
U.S. Nano 40nm (cyclohexane/OA)	3.2642	680	20.23	90.867	176.16	57.5
Novacentrix 80nm (RP-2/OA)	2.8621	580	24.94	84.056	162.96	28.9

CONSIDERATION OF FURTHER PROCESSING

In order to make economic use of commercially sourced material, it will be necessary to develop a method for rapid segregation of the large particle fraction that requires further processing. This could be performed by timed gravitational sedimentation or timed centrifugation if faster action is needed (can easily generate 100 – 1000 g). Once segregated, the larger particles (hopefully consisting mainly of agglomerates of much smaller primary particles, instead of single large primary particles; this will need to be assessed on a per-material basis) must be broken down to the appropriate size. Traditional particle processing techniques such as sonication or mechanical milling can be problematic for aluminum; due to aluminum’s low melting point, sonication can actually cause “welding” of previously non-bonded particles due to concentration of the sonic energy at contact points, and mechanical milling can greatly distort the particle shape due to aluminum’s ductility. Therefore, alternative techniques should be considered.

- For brittle particles and/or loosely-bound agglomerates, high-shear mixing (for example, the “Dispersator” mixer²⁹ has been used by the investigators previously) should be effective.
- Cryo-milling may be necessary for Al particles since they are ductile at ambient temperatures, and are not expected to break up cleanly.

SUMMARY & CONCLUSIONS

A wide variety of particles and dispersants were considered. Based on availability, performance, and suitability for the application, a limited set were selected for further evaluation. Qualitative screening techniques and procedures were developed to relatively quickly and easily evaluate the dispersion characteristics of various nanoparticles with selected dispersant materials. Aluminum nanopowders from two different manufactures were further investigated with two different dispersing agents; the effect of dispersant concentration and solvent was tested. To remove excessively large agglomerates (for this application) found in all the commercial particles examined, the mixtures were filtered and the resulting suspension characterized for particle size distribution and stability. The following conclusions and lessons learned can be drawn from this work:

- Methods have been developed to allow relatively quick and inexpensive qualitative evaluation of the compatibility and dispersion potential of both dispersants and nanopowders.
- Dispersants: Oleic acid appears suitable as dispersant for Al and possibly Ti nanopowders. Iso-stearic acid-N appears to be somewhat less effective than oleic acid for aluminum nanoparticles, but may still be useful.
- Materials: All commercially available nanoparticles examined appear to have a significant fraction of non-readily dispersible particles larger than the size limit for stable colloidal suspensions (according to the stability boundary determined by settling calculations)
 - As-delivered particles contain a significant fraction in non-chemically dispersible and/or “hard” agglomerates that will require mechanical processing and/or deletion;
 - Filtration of suspensions can be used to generate more stable suspensions by removing particles of sizes that will settle out, but this will result in unacceptably high mass losses for the highly agglomerated commercial materials examined;

- Therefore, multi-step processing will be necessary when using nanoparticles from commercial sources for formulation of nano-fluid fuels.

ACKNOWLEDGMENTS

The work reported in this paper was performed as a fundamental research task under a subcontract to the Pennsylvania State University from Combustion Propulsion & Ballistic Technology Corporation, serving as the prime contractor for a U. S. Air Force Small Business Innovative Research Phase I program, Contract No. FA9300-13-M-1008.

REFERENCES

- ¹ Sutton, G. P. and Biblarz, O., **Rocket Propulsion Elements, Seventh Edition**, John Wiley & Sons, Inc., New York, NY, 2001., p.496.
- ² Gordon, S. and McBride, B. J., "Computer Program for Calculation of Complex Chemical Equilibrium Compositions and Applications I. Analysis," NASA RP-1311, National Aeronautics and Space Administration - Lewis Research Center, Cleveland, OH, October 1994.
- ³ Risha, G. A., Boyer, E., Evans, B., Kuo, K. K., and Malek, R., "Characterization of Nano-Sized Particles for Propulsion Applications," *Material Research Society Symposium Proceedings*, Materials Research Society, 2004, pp. AA6.6.1 – AA6.6.12.
- ⁴ Tepper, F., and Kaledin, L. A., "Combustion Characteristics of Kerosene Containing ALEX Nano-Aluminum," *International Journal of Energetic Materials and Chemical Propulsion*, vol. 5, 2002, pp. 195–205.
- ⁵ Jones, M., Li, C. H., Afjeh, A., and Peterson, G., "Experimental study of combustion characteristics of nanoscale metal and metal oxide additives in biofuel (ethanol).," *Nanoscale research letters*, vol. 6, Jan. 2011, p. 246.
- ⁶ Gan, Y. and Qiao, L., "Combustion characteristics of fuel droplets with addition of nano and micron-sized aluminum particles," *Combustion and Flame*, vol. 158, Feb. 2011, pp. 354–368.
- ⁷ Gan, Y., Lim, Y. S., and Qiao, L., "Combustion of nanofluid fuels with the addition of boron and iron particles at dilute and dense concentrations," *Combustion and Flame*, Vol. 159, Apr. 2012, pp. 1732–1740.
- ⁸ Sabourin, J. L., Yetter, R. A., Asay, B. W., Lloyd, J. M., Sanders, V. E., Risha, G. A., and Son, S. F., "Effect of Nano-Aluminum and Fumed Silica Particles on Deflagration and Detonation of Nitromethane," *Propellants, Explosives, Pyrotechnics*, vol. 34, Oct. 2009, pp. 385–393.
- ⁹ Sabourin, J. L., Dabbs, D. M., Yetter, R. A., Dryer, F. L., and Aksay, I. A., "Functionalized Graphene Sheet Combustion," *ACS Nano*, Vol. 3, 2009, pp. 3945–3954.
- ¹⁰ Allen, T., **Particle Size Measurement, 4th ed.**, Chapman and Hall, New York, NY, 1990, p. 259.
- ¹¹ Moore, D. W. and Orr, Jr., C., "The influence of diffusion on sedimentational particle size analysis," *Powder Technology*, Vol. 8, 1973, pp. 13-17.
- ¹² Adair, J. and Boyer, E., manuscript in preparation for *Journal of Colloid and Interface Science*.
- ¹³ FEI Nova™ NanoSEM 630
- ¹⁴ Risha, G. A., et al., "Combustion of nano-aluminum and liquid water," *Proceedings of the Combustion Institute*, Vol. 31, 2007, pp. 2029–2036.
- ¹⁵ Young, G. Y., et al., "Combustion characteristics of boron nanoparticles," *Combustion and Flame*, Vol. 156, 2009, pp. 322–333.
- ¹⁶ Shuqing, S. and Leggett, G. J., "Micrometer and Nanometer Scale Photopatterning of Self-Assembled Monolayers of Phosphonic Acids on Aluminum Oxide," *Nano Letters*, Vol. 7, No. 12, 2007, pp. 3753-3758.
- ¹⁷ Cordero, et al., "Surface Changes of Alumina Induced by Phosphoric Acid Impregnation," *Applied Catalysis*, Vol. 56, 1989, pp. 197-206.
- ¹⁸ Van Devener, B., et al., "Oxide-Free, Catalyst-Coated, Fuel-Soluble, Air-Stable Boron Nanopowder as Combined Combustion Catalyst and High Energy Density Fuel," *Energy & Fuels*, Vol. 23, 2009, pp. 6111–6120.

- ¹⁹ Gonzalo-Juan, I., McBride, J. R., and Dickerson, J. H., "Ligand-mediated shape control in the solvothermal synthesis of titanium dioxide nanospheres, nanorods and nanowires," *Nanoscale*, Vol. 3, 2011, pp. 3799-3804.
- ²⁰ Mousavand, T., et al., "Organic-ligand-assisted supercritical hydrothermal synthesis of titanium oxide nanocrystals leading to perfectly dispersed titanium oxide nanoparticle in organic phase," *Journal of Nanoparticle Research*, Vol. 9, 2007, pp. 1067–1071.
- ²¹ Sahoo, P. K., et al., "Synthesis of tungsten nanoparticles by solvothermal decomposition of tungsten hexacarbonyl," *International Journal of Refractory Metals and Hard Materials*, Vol. 27, No. 4, July 2009, pp. 784–791.
- ²² Babushok, V. I. and Tsang, W., "Influence of Phosphorus-Containing Fire Suppressants on Flame Propagation," International Conference on Fire Research and Engineering (ICFRE3), Third (3rd). Proceedings. Society of Fire Protection Engineers (SFPE), National Institute of Standards and Technology (NIST) and International Association of Fire Safety Science (IAFSS). October 4-8, 1999, Chicago, IL, Society of Fire Protection Engineers, Boston, MA, 1999, pp. 257-267.
- ²³ van der Veen, I. and de Boer, J., "Phosphorus flame retardants: Properties, production, environmental occurrence, toxicity and analysis," *Chemosphere*, Vol. 88, No. 10, 2012, pp. 1119–1153.
- ²⁴ <<https://www.nissanchem-usa.com/products/fineoxocol/>>, accessed December 11, 2014.
- ²⁵ <<http://www.pall.com/main/laboratory/product.page?lid=gri78m6h>>, accessed December 12, 2014.
- ²⁶ Outcalt, S. L, Laesecke, A., and Brumback, K. J., "Thermophysical Properties Measurements of Rocket Propellants RP-1 and RP-2," *Journal of Propulsion and Power*, Vol. 25, No. 5, September–October 2009, pp. 1032-1040.
- ²⁷ Adair, J. H., et al., "Colloidal Lessons Learned for Dispersion of Nanosize Particulate Suspensions," in **Lessons in Nanotechnology from Traditional and Advanced Ceramics**, Proceedings of the World Academy of Ceramics, J.F. Baumard (ed.), Techna Group Srl, Faenza, Italy, 2005, pp. 93-145.
- ²⁸ Allen, T., **Particle Size Measurement: Powder Sampling and Particle Size Measurement, Vol. 1, 5th ed.**, Chapman & Hall, London, 1997.
- ²⁹ See <http://www.halliburton.com/fann/products/supplies-and-reagents/lab-equipment-supplies/blenders-and-mixers/shearers.page> (accessed March 20, 2014).